Full scale laboratory tests of timber-concrete composite bridges

Daniel Harrach
Department of Structural and Geotechnical Engineering
Széchenyi István University
Győr, Hungary
harrach.daniel@sze.hu

Majid Movahedi Rad
Department of Structural and Geotechnical Engineering
Széchenyi István University
Győr, Hungary
majidmr@sze.hu

***Abstract*—This article presents two 6.0 m span custom-designed timber-concrete composite bridge structures subjected to both concentrated and distributed loads. The bridge structures were designed as glue-laminated timber girders connected with reinforced concrete bridge deck with shear connections. The first bridge model has two glue-laminated timber girders, while the second one has six girders. To verify the behavior of the designed structure, we built a full-scale experimental structure and performed a load test. In the laboratory tests, the serviceability limit states, standard loads and load arrangements were investigated. The results of the loading experiments were evaluated. The bridge structures in this article will be placed outdoors after completion of the tests, where they will be used as pedestrian-bicycle bridges.**

Keywords*— *Timber-concrete structures, composite structures, bridge model, static load

I. Introduction

In the 21st century, perhaps the most important aspect in bridge construction is no longer applied to meet the requirements of functional needs where the aspects of structure selection do not determine the traffic requirements alone. In addition to load-bearing capacity, durability and economy are the most important design considerations, but aesthetics and environmental awareness have always been important in the design of modern bridges and structures.

Timber-concrete composite bridges are widespread in the western and northern parts of Europe [1]. In the case of timber bridges with a lifespan of more than 30 years and wooden structures with insufficient load-bearing capacity, the idea to reinforce the wooden beams with a concrete slab first came to light. Timber-concrete composite (TCC) structures produced using two elements (tensioned wooden beam and compressed reinforced concrete slab) where composite structures can be considered as modern structures [2]. Wood is a natural/renewable building material and reinforced concrete is a modern building material. In this work, the timber beams are located in a protected place under the reinforced concrete slab, which protects the wood from the swelling effects caused by precipitation. [3]

To use wood and concrete as a composite structure, it is necessary for the elements to work together. Ensuring adequate relationship rigidity is the main goal that is able to transfer shear forces at the connected part of the structure [4, 5]. However, it is important to note that joining timber and concrete does not mean joining two perfectly rigid materials. The coupling element can also turn, slip or pull out in the wood and concrete parts [6]. Both wood and concrete have time-dependent properties (shrinkage, swelling, permanent deformation), in the case of design an optimal connection, the coupling element must also be able to absorb the resulting additional stresses [7].

In order to achieve an optimal wood-concrete composite behaviour, the neutral axis must be located in the vicinity of the contact plane. [8] The stiffness ratio and the strength of the materials show that the ratio of the optimal structural element thickness between timber and concrete should be around 1:10 [9]. However, this ratio is not economical in the case of small bridge structures because the design standards and design regulations prescribe a minimum reinforced concrete slab thickness of 15-20 cm depending on the structural variation [10]. In order to reduce the structural height, the timber beams are provided with carbon fiber reinforcement at the tensioned side and as a result, the beam's height can be significantly reduced [11].

Load tests of full-size models of wood-concrete bridges were investigated only in [12], where GLT beams with precast bridge deck segments made of ultra-high-performance concrete without reinforcing bars.

In this paper, we deal with the static load tests of two full-size (6,0 m span, 2,4 m width) bridge models performed under laboratory conditions. The special feature of the designed TCC bridges, that they have been designed in such a way that they can be used as an actual pedestrian-bicycle bridge with minimal reconstruction. During the design of the experimental program, it was important to match the bridge structures to the real traffic loads. Dynamic load tests will take place at a later stage of the research project.

II. Experimental program

A. Models

Two timber-concrete composite (TCC) bridges were made with dimensions of 6.5 m bridge length, 6.0 m span, and 2.4 m track width (without parapet). The first bridge has two glue-laminated timber (GLT) girders design (TC-A), while the second has six GLT girders (TC-B). The shear connection between the timber and the concrete is given by a perforated steel plate connection glued into the timber beams along its entire length and the shear elements were connected to the reinforcement of the reinforced concrete traffic deck. The ends of the timber girders are also connected to the cross girder with the same connection type described previously as it can be seen at the left side of the Figure 1.

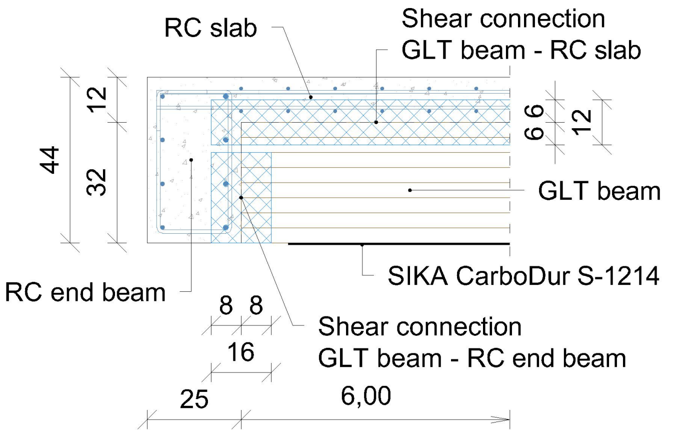

Fig. 1. The connection system between the GLT beam and the RC elements

Since the case of a connection between concrete and wood, the wood extracts water from the concrete and reduces the strength of the concrete near the connection, a separation layer was built between the timber and the concrete parts in order to separate the water from the wood during the setting of the concrete. The tensioned side of the timber beams was reinforced with CFRP strips to reduce the required structural height of the bridge models. Table I provides the properties of the materials used.

Figure 2. shows the cross-section of the TC-A bridge model which has 12 cm reinforced concrete desk, and two GLT beams 16x32 cm, also two shear connections were placed between the timber beam and the reinforced concrete slab.

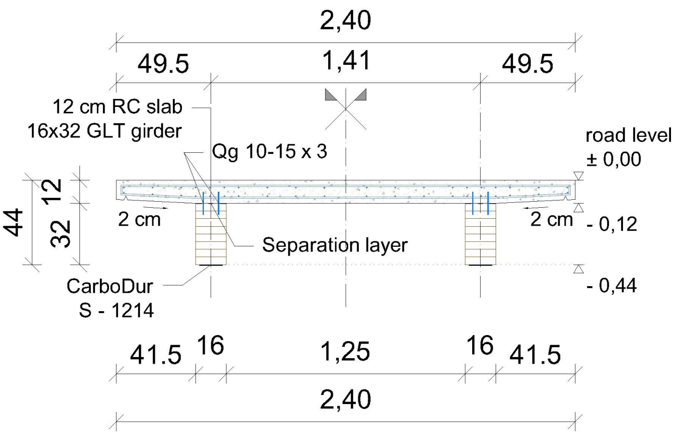

Fig. 2. Cross-section of the two girders bridge model (TC-A)

In the case of the six-girders design (TC-B), the thickness of the traffic deck is 8 cm, the timber beams are made with a 12x24 cm cross-sections as shown in Figure 3.

TABLE I. MATERIALS PROPERTIES

Material		Com-pression strength f_c [N/mm²]	Tensile strength f_t [N/mm²]	Modulus of elasticity E [N/mm²]
Concrete	C35/45	35	3,20	34.000
Rebar	B500B	560	560	200.000
CFRP	SIKA CarboDur S-1214	-	3.1000	170.000
Epoxy glue	SikaDur 30	-	26-30	11.200
Perforated steel plate	Qg 10-15-3 S355J	85-95	510-680	210.000
Injection	SikaDur-52 Injection	52	37	1.800

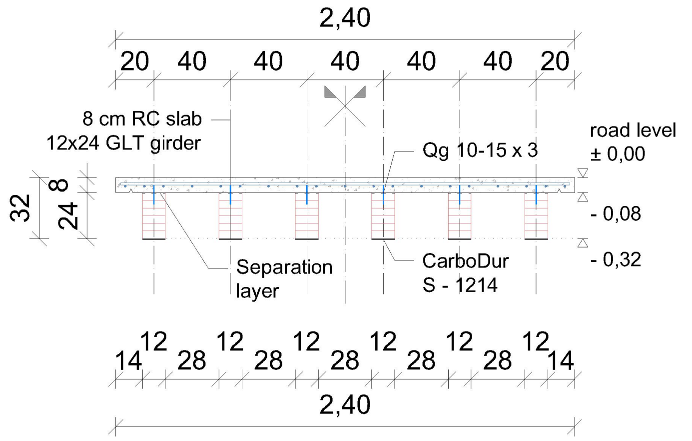

Fig. 3. Cross-section of a six girders bridge model (TC-B)

B. Loading process

Several loads were applied to the bridge models in order to simulate the actual behavior. However, the load-bearing limit of the structures could not be reached and the bridges did not load up to failure as the investigation was in operating condition. During the loading process, we followed the regulations of Eurocode [13] and e-UT [14] standards where the aim was to prove the resistance for the standard loads. The bridge models will be installed in an external site after the laboratory test period as these bridges will be pedestrian-bicycle bridges and according to the planned location, we dealt with the load required for pedestrian-bicycle bridges according to EN 1991-2 [13]

- Distributed load: Load Model No. 1:

Recommended characteristic value for pedestrian traffic areas and bicycle lanes of short or medium-length footbridges:

$$q_{fk} = 5{,}0\ kN/m^2 \quad (1)$$

- Concentrated load: Load Model No. 2:

To test the-local effects, a vertical force shall be applied to a surface of 0,1 x 0,1 m:

$$Q_{f,wk} = 10\ kN \quad (2)$$

- Service Vehicle Load: Load Model No. 3:

Figure 4 shows the standard load arrangement of the service vehicle according to EC. The arrow indicates the direction of travel of the vehicle.

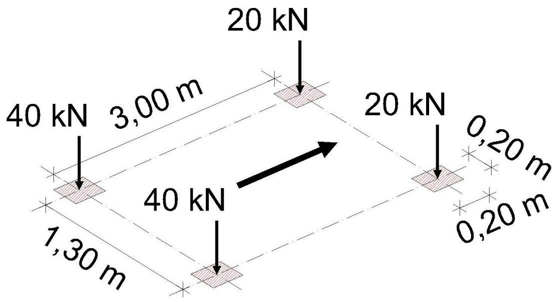

Fig. 4. Vertical load model of the service vehicle

Concerning the case of distributed load at an area, different load arrangements have been investigated:

- Full loading (Full)
- Full loading over half the length (Uni)
- One-sided full loading (Lane)
- Checkerboard loading (Chess)

The distributed loading was applied by placing sandbags at the loading area considering load steps of 100 kg/m^2 (0,1 kN/m^2). In each case, the maximum load value was reached in 5 load steps. Figures 5 and 6 show typical arrangements for the distributed loads.

Fig. 5. Load arrangements for distributed load (Chess_1)

Fig. 6. Load arrangements for distributed load (Lane_2)

In the case of concentrated forces, the following types were examined separately:

- Load on the major axle of the service vehicle (40 kN)
- Total load of the service vehicle (40+20 kN) at maximum bending stress location
- Service vehicle's full load in the middle of the field with 1,5 times safety factor
- Load of one wheel of service vehicle at the center of the field, at the end of the console
- Load model No. 2 in the middle of the field, in the axle of the bridge.

Axle and wheel loads were tested with forces acting on standard surfaces. Figures 7 and 8 show the test setups of the concentrated loading period of the models.

Fig. 7. Axle load arrangements during concentrated load (S_2)

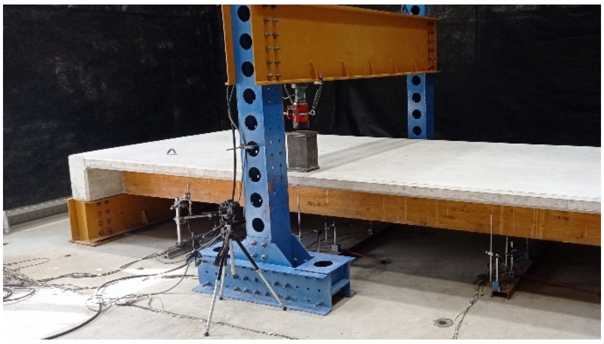

Fig. 8. Wheel load arrangements during concentrated load (A_4)

The vertical deflection of the bridges was measured in three different cross-sections at a total of fifteen measuring points during the whole loading process.

III. Test Results

During the load tests, the deflections resulting from the self-weight of the bridges were not measured separately, only the deflections due to overload were recorded. The load-displacement diagrams obtained during loading showed linear behavior for all measurement points. Besides, the magnitudes of the largest deflection values correspond to the results obtained during the modeling. Figures 9 and 10 shows the shape of the structure as the maximum load value was reached in different representations.

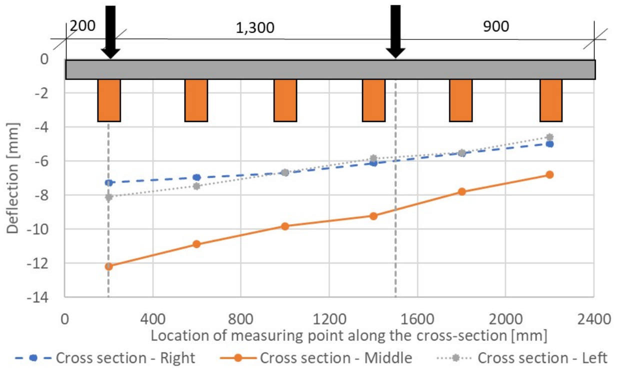

Fig. 9. Deflection diagram of the TC-B bridge model under the effect of the total load of the service vehicle in nonsymmetrical arrangements (S_3)

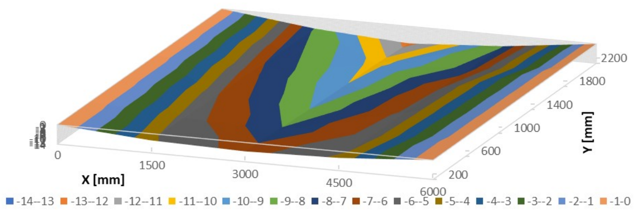

Fig. 10. Contour line map of the TC-A bridge model under right-hand eccentric loading at the middle of the bridge (A_2).

During the eccentric loads, the deformed shape is clearly outlined and due to the linear transverse behavior, it can be said that the main girders of the bridges cooperated with the reinforced concrete slab.

Figure 11 shows how the behavior of the structure along different measurement axes developed longitudinally. Where the different colors shows the position of measurements on the cross-section.

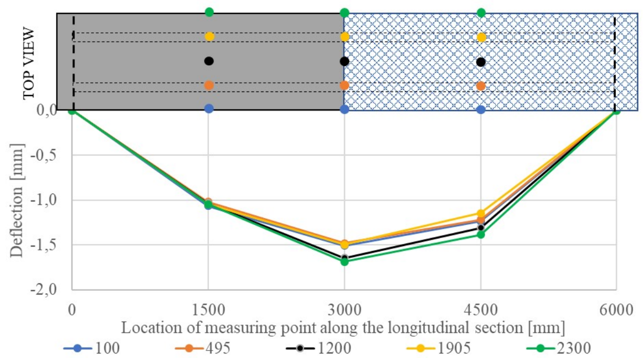

Fig. 11. Deflection diagram of the TC-A bridge model along the longitudinal section of the girder in the case of one-sided full loading (Uni_2).

Table II. shows the maximum measured deflection values for TC-A and TC-B bridges under different concentrated loads. For sure, the maximum measured value was not in the same place for the different load cases. The load A_1 to A_4 refers to the asymmetrical load positioning along the bridge model length, the load types S_1 to S_4 refers to the symmetrical concentrated load arrangement.

TABLE II. EXPERIMENTAL TEST RESULTS FOR CONCENTRATED LOAD

Load type	Load location	Eccentricity of load	Load	Deflection	
				TC-A	TC-B
	d_x [mm]	d_y [mm]	F_{max} [kN]	e_{max} [mm]	e_{max} [mm]
A_1	2500	0	2x60 kN t=1,30 m	**7,78**	**9,66**
A_2	2500	+350		**9,21**	**12,53**
A_3	2500	-350		**9,36**	**12,29**
A_4	2500	-1000	1x60kN	**5,62**	**8,67**
S_1	3000	0	2x40 kN t=1,30 m	**4,76**	**6,67**
S_2	3000	+350		**6,11**	**8,26**
S_3	3000	-350		**6,03**	**8,12**
S_4	3000	-1000	1x40kN	**5,75**	**5,91**

Table III. shows the maximum measured deflection values for TC-A and TC-B bridges under different distributed loads. An indexed load of "_2" means an inverse arrangement of an indexed load of "_1".

TABLE III. EXPERIMENTAL TEST RESULTS FOR DISTRIBUTED LOADS

Load type	Load	Deflection	
		TC-A	TC-B
	q_{max} [kN/m^2]	e_{max} [mm]	e_{max} [mm]
Full	5,0	**2,68**	**3,54**
Chess_1	5,0	**1,42**	**1,89**
Chess_2	5,0	**1,49**	**1,93**
Uni_1	5,0	**1,89**	**1,89**
Uni_2	5,0	**1,91**	**1,97**
Lane_1	5,0	**2,93**	**2,64**
Lane_2	5,0	**2,89**	**2,78**

Based on the results of the tests, both bridge structures remained in the operating load level due to the load as no permanent deformations have occurred. Most importantly, it was possible to compare the maximum deflection values by the standards e-UT 07.01.12 [15] and EN 1995:2:2014 [13] prescribes the limit for the maximum deflection of footbridges due to traffic loads as follows:

$$L/400 = 15{,}625\ mm > e_{max} \quad (3)$$

As it can be seen in Table II. and Table III., the tested bridge's deflection value did not occur even in the case of the critical load arrangements.

SUMMARY

This paper presents static load tests of timber-concrete composite bridge models. Where the behavior of two and six main girder structures under concentrated and distributed loads was examined. The main aim of this research was to investigate the bridge models under standard loads. After the investigation period, the models will be functional bridges at an external site. Under the bridge standard loads, the structures were adequate, after conversion to road regulations (placing pedestrian parapets, application of the anti-slip coating,…), are suitable to prove against actual traffic. The bridges will be equipped with a monitoring system at the actual installation site that providing an opportunity to compare laboratory tests and on-site results, and to describe the behavior of the structures as accurately as possible.

References

[1] Rodrigues J., Dias A., Providência P.: Timber-Concrete Composite Bridges: State-of-the-Art Review, BioResources Vol 8, No. 4, 2013. pp 6630-6649.

[2] Fragiacomo, M.: Experimental behaviour of a full-scale timber–concrete composite floor with mechanical connectors, Mater Struct: 45(11), 2012, pp 1717–1735.

[3] Bajzecerová V., Kanócz J.: The Effect of environment on Timber-Concrete Composite Bridge Deck, Procedia Engineering 156, 2016, pp. 32-39.

[4] Cecotti, A.: Timber-concrete composite structures, In: Blass H. (Ed) Timber Engineering, step 2, Centrum Hout, The Netherlands, 1995.

[5] J. N. Rodrigues, A. M. P. G. Dias, P. Providencia: Timber-concrete composite bridges: state-of-the art review, 2013, BioResources 8(4), pp 6630–6649.

[6] L. S. A. S. Samuel, C. Aucliar: Simplified nonlinear model for timber-concrete composite beams, International Journal of Mechanical Sciences, 2016, 1. kötet 117, pp 30-42.

[7] Dias, A. M. P. G.: Mechanical behavior of timber-concrete joints, PhD Thesis, University Coimbra, Portugal, 2005.

[8] Gutkowski, R., Brown, K., Shigidi, A., Natterer, J.: Laboratory tests of composite wood–concrete beams, Construction and Building Materials 22., 2008, pp 1059–1066.

[9] Negrão, J. H. J. O., Oliveira, F. M. M., Oliveira, C. A. L., Cachim, P. B.: Glued Composite Timber-Concrete Beams. II: Analysis and Tests of Beam Specimens, Journal of Structural Engineering 136., 2010, pp 1246-1254.

[10] e-UT 07.01.14:2011: Beton, vasbeton és feszített vasbeton hidak. Közúti hidak tervezése (KHT) 4., Magyar Útügyi Társaság

[11] Kim, Y. J., Harries K. A.: Modelling of timber beams strengthened with various CFRP composites, Engineering Structures: 32, 2010, pp 3225–3234.

[12] Holý M., Cˇítek D., Tej P., Vráblík L.: The Experimental Timber–UHPC Composite Bridge, Sustainability 13, 4895, 2021.

[13] EN 1995-2:2014: Eurocode 5: Design of timber structures - Part 2: Bridges

[14] EN 1991-2:2006: Eurocode 1: Actions on structures - Part 2: Traffic loads on bridges

[15] e-UT 07.01.12:2011: Erőtani számítás. Közúti hidak tervezése (KHT) 2., Magyar Útügyi Társaság